

# Adaptively controlled supercontinuum pulse from a microstructure fiber for two-photon excited fluorescence microscopy

Junji Tada, Taiki Kono, Akira Suda, Hideaki Mizuno, Atsushi Miyawaki, Katsumi Midorikawa, and Fumihiko Kannari

Selective fluorescence excitation of specific molecular species is demonstrated by using coherent control of two-photon excitation with supercontinuum pulses generated with a microstructure fiber. Pulse shaping prior to pulse propagation through the fiber is controlled by a self-learning optimization loop so that the highest fluorescence signal contrast between two fluorescent proteins is obtainable. The self-learning optimization loop successfully controls both the optical nonlinearity of the microstructure fiber and the two-photon excitation of the fluorescent proteins. © 2007 Optical Society of America

OCIS codes: 320.2250, 320.550, 320.7110.

## 1. Introduction

Multiphoton excited fluorescence microscopy using femtosecond lasers provides us with remarkable advantages in 3D imaging of biosamples, such as higher spatial resolution, background-free signal, better penetration in thick samples, and reduced out-of-focus photobleaching and phototoxicity. Recently, pulse-shaping technology for femtosecond laser pulses,<sup>1</sup> allowing control of the phase and amplitude of a discrete number of frequency modes across the bandwidth of femtosecond laser pulses, has revolutionized the various types of experiments on nonlinear optical interactions of laser fields with matter. Selective fluorescence microscopy has also been demonstrated through the selective excitation of different fluorescent probes by designing the  $n$ th-order electric field of the laser with the pulse-shaping technique.<sup>2-4</sup> Since the two-photon excited fluorescence is simply proportional to the over-

lap integral between the second-harmonic (SH) spectrum and the two-photon excitation spectrum of the chromophore,<sup>2-5</sup> a chromophore with different excitation spectra can be selectively excited by shaping the SH spectrum. Pulse shapers together with computer controlled self-learning algorithms<sup>6</sup> have also been used to maximize the two-photon fluorescence efficiency defined by the fluorescence signal power divided by the SH power of the pumping laser.<sup>7</sup> Note that the Fourier transform limited (FTL) pulse always produces the highest multiphoton fluorescence intensity, but the highest efficiency is achieved by complex shape pulses that is difficult to interpret. The optimal pulse shapes reduce the photobleaching in the two-photon excitation of the enhanced green fluorescence protein (EGFP).<sup>7</sup>

Based on conventional single femtosecond laser sources, current implementation permits selective excitation over the bandwidth of  $\sim 100$  nm or less. Extending this range is desirable to access various chromophores. Spectral phase shaping of the supercontinuum generated by a microstructure fiber (MSF) will be a possible solution without multiple laser sources. Parametric four-wave-mixing processes can easily be phase matched near zero group-velocity dispersion (GVD), thus spectral broadening is enhanced, extending all the way from  $\sim 400$  nm to  $\sim 1.5$   $\mu$ m with 110 fs laser pulses launched into a 75 cm long MSF.<sup>8</sup> Supercontinuum pulses have been employed for nonlinear spectroscopy, including ultrafast pump and probe techniques and implementations of coherent anti-Stokes Raman scattering (CARS). So far, in most

---

J. Tada, T. Kono, and F. Kannari (kannari@elec.keio.ac.jp) are with the Department of Electronics and Electrical Engineering, Keio University, 3-14-1, Hiyoshi, Kohoku-ku, Yokohama 223-8522, Japan. A. Suda and K. Midorikawa are with the Laser Technology Laboratory, RIKEN, 2-1, Hirosawa, Wako, Saitama 351-0198, Japan. H. Mizuno and A. Miyawaki are with the Laboratory for Cell Function Dynamics, Brain Science Institute, RIKEN, 2-1, Hirosawa, Wako, Saitama 351-0198, Japan.

Received 24 October 2006; revised 9 January 2007; accepted 11 January 2007; posted 12 January 2007 (Doc. ID 76364); published 1 May 2007.

0003-6935/07/153023-08\$15.00/0

© 2007 Optical Society of America

of experiments the spectral phase of the continuum pulse was left unmodified.<sup>9–13</sup> Some effort has been made to compensate for phase dispersion and generate extremely short pulses from the ample bandwidth available. Recently, the pulse-shaping technique has been applied to control the spectral phase of supercontinuum pulse for coherently controlled CARS microspectroscopy.<sup>14</sup>

In this paper we employ supercontinuum pulses for two-photon excited fluorescence microscopy. To compress the continuum pulse, a simple computer controlled self-learning optimization scheme can be used with the total integrated signal of SH power of the continuum pulse as single feedback value. Then one can design SH spectra of the continuum pulse by the same procedure developed for femtosecond laser pulses to selectively excite specific two-photon excitation. In our scheme, however, we place a computer controlled pulse shaper prior to pulse propagation in the MSF. There are two advantages in this scheme. First, a  $4f$  pulse shaper that employs a segmented spatial light modulator is known to be a spatiotemporal coupling system that changes the output spatial profile as well as the temporal profile when the spectrum is filtered to manipulate temporal waveforms.<sup>15,16</sup> To fully characterize the shaped optical field and interpret light–matter interactions, one must take into account the profile in both space and time. Thus far, no one has considered the influence of the spatiotemporal coupling in the multiphoton excited fluorescence spectroscopy using shaped femtosecond laser pulses. In fact, it is not easy to fully analyze the spatiotemporal profile near the focus in a chromophore sample. In our scheme, where the pulse shaping is done before pulse propagation in the MSF, the spatial mode is always controlled by the single-mode fiber. Therefore we can ignore the spatiotemporal coupling issue in the multiphoton excitation. Second, we can use a MSF as a flexible light guide to deliver the shaped broadband laser pulse to a fluorescence microscope.

The supercontinuum spectra generated with MSFs are changed by the spectral phase modulation of the input laser pulse.<sup>17–20</sup> In our previous study, we showed that any regions of the continuum spectral power can be enhanced by employing a computer controlled optimization loop.<sup>20</sup> In this paper we demonstrated selective two-photon excitation of fluorescent proteins by adaptively shaping the supercontinuum spectrum generated from MSFs.

## 2. Experiment

The experimental setup is shown in Fig. 1. A mode-locked Ti:sapphire laser (Mira-Seed, Coherent Inc., Santa Clara, Calif., USA) was used as the light source, which provides pulses at a repetition rate of 76 MHz, with a central wavelength of 800 nm, a pulse duration of 32 fs, and an average power of  $\sim 500$  mW. The spectral phase of the laser pulses was modulated with a  $4f$  pulse shaper consisting of 600 line gratings, Fourier lenses, and a liquid crystal spatial light modulator (SLM) (LC-SLM-128, Cambridge

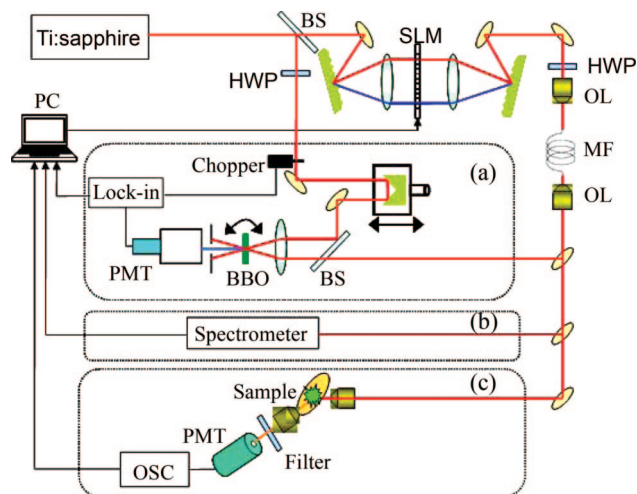


Fig. 1. (Color online) Schematic of experimental setup. (a) XFROG setup to characterize supercontinuum pulses. (b) Output of a fiber-coupled spectrometer is sent to a PC to enhance a specific spectral band of supercontinuum pulse with self-learning adaptive control. (c) Two-photon excitation of chromophore. The fluorescence power is sent to the PC to adaptively optimize the excitation pulse shape.

Research and Instrumentation, Woburn, Mass., USA), which has individually controllable 128 pixels. The shaped pulse is launched into the 35 cm long MSF-A (NL · 2.0 · 770, Crystal Fibre A/S, Birkerød, Denmark). The clad and core diameters are  $150 \pm 3$  and  $2.00 \pm 0.2$   $\mu\text{m}$ , respectively. The zero GVD wavelength is  $770 \pm 20$  nm. In the third experiment, we also used the 30 cm long MSF-B made by Mitsubishi Densen Co., Tokyo, Japan. The fiber core diameter is  $3.06$   $\mu\text{m}$ . The zero GVD wavelength is 820 nm. The laser coupling efficiency to the MSFs is typically  $\sim 20\%$ .

In the first experiment, we examined the closed-loop controllability of a supercontinuum spectrum by the input laser pulse shape. We measured the spectrum of the supercontinuum generated from the MSF with a spectrometer and fed back the integrated difference in the spectral shape from the target spectrum shape to the SLM. We used the simulated annealing (SA) method as a learning algorithm.<sup>21</sup> During the experiment, we produced an FTL pulse at the input of the MSF using the self-learning closed-loop optimization so that the SH power becomes highest. In the second experiment we used three different dye solutions to demonstrate that the adaptive pulse shaping can enhance the two-photon excited fluorescence of each dye solution. We employed the cross frequency resolved optical gating (XFROG) method to characterize the optimal supercontinuum pulse using a 300  $\mu\text{m}$  thick  $\beta$ -barium borate (BBO) crystal. We used an unshaped laser pulse split before pulse shaping as a reference pulse. The sum frequency spectra of the supercontinuum pulse and the reference pulse were detected with a monochromator and a photomultiplier as a function of relative time delay. The time resolution was approximately 8.3 fs. Since our BBO crystal is too thick to simultaneously monitor

the broadband sum frequency spectra generated by the supercontinuum, the phase matching angle of the BBO was adjusted every time for each sum frequency measurement. In the third experiment, two fluorescent proteins, EGFP and enhanced cyan fluorescence protein (ECFP) were simultaneously excited by the same supercontinuum pulse. The concentration of the fluorescent protein solutions is 53.3 mg/cc and 30.0 mg/cc for EGFP and ECFP, respectively. The peak absorption cross section is located at 484 and 434 nm for EGFP and ECFP, respectively. The two-photon excited fluorescence is monitored by separate photomultipliers and proper bandpass filters. The transmission band of the bandpass filter is 500–541 nm and 464–500 nm for EGFP and ECFP, respectively. Then the fluorescent signal ratio EGFP/ECFP is used as single feedback value to control the pulse shaper.

### 3. Results and Discussion

#### A. Adaptive Control of Supercontinuum Spectrum

We targeted the spectral bands located in the supercontinuum spectrum generated by the FTL input laser pulse and controlled the input laser pulse shape so that the spectral power in the targeted band is maximized. The average power of the supercontinuum is  $\sim 1.5$  mW. We calculated the ratio of spectrum power concentrated in the targeted spectral band relative to the entire supercontinuum spectrum power detected by the spectrometer and used the power ratio as a control parameter of the SA algorithm. In the SLM, we set the phase gray level as 16. Thus the minimum spectral phase variation at designing a phase-only shaping mask is  $2\pi/16$  rad. The result of this adaptive control is shown in Fig. 2. The supercontinuum obtained when the input pulse without any spectral phase modulation was launched to the MSF-A is shown at the top. The initial input pulse with a null phase mask is not a FTL pulse because of the dispersion of various optics placed before the

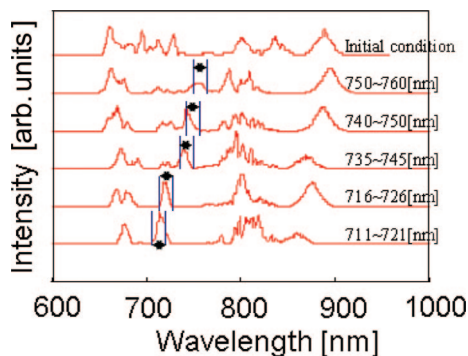


Fig. 2. (Color online) Adaptively shaped supercontinuum spectra plotted in the linear scale. The marked spectral band of each spectrum was targeted to be enhanced by shaping the femtosecond laser pulse launched into the microstructure fiber. The supercontinuum spectrum obtained by the unshaped input laser pulse with a null spectral phase mask is shown in the top. The average power of the supercontinuum pulses is  $\sim 1.5$  mW.

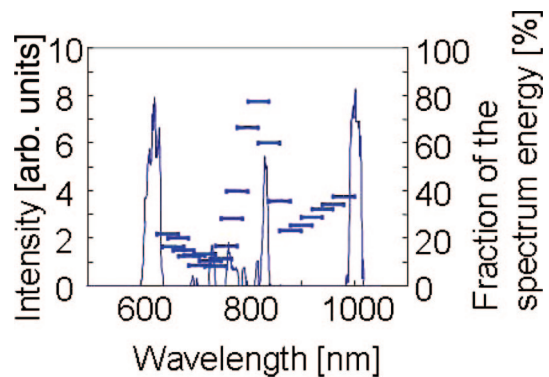


Fig. 3. (Color online) Plots of the fraction of spectral powers concentrated into the various targeted spectral bands by adaptive pulse shaping. The background spectrum is the supercontinuum spectrum (linear scale) obtained by the FTL laser pulse. The average power of the supercontinuum pulses is  $\sim 6.5$  mW.

pulse shaper, such as lenses and an isolator. We targeted the spectral bands located between the anti-Stokes Raman peak at approximately 650 nm and the pump pulse at 711–721, 716–726, 735–745, 740–750, and 750–760 nm. All the spectral powers of the targeted spectral bands were successfully enhanced compared with those in the supercontinuum spectrum generated by the pulse with the null phase mask.

Figure 3 shows the summary of the series of experiments. The fraction of spectral powers concentrated into the various targeted spectral bands by adaptive pulse shaping is plotted. The solid curve indicates the supercontinuum spectrum (linear scale) obtained by the FTL pulse. The total supercontinuum power was  $\sim 6.5$  mW during this series of experiments. The entire spectrum extended all the way from 600 to 1000 nm. The spectral bands around the central wavelength of the input pulse show the higher enhancement factor. Relatively efficient energy concentration is attained also near the Stokes and anti-Stokes components at the spectral wings. It should be emphasized that the optimization control to concentrate the optical energy into a distinct spectral region of the supercontinuum does always affect other parts of the spectrum. We demonstrated the energy concentration into a specific spectral region with higher supercontinuum powers up to 20 mW.<sup>20</sup> At higher input energies, the spectral energy at approximately the 800 nm excitation pulse is still strong. Therefore, for practical use, it may be necessary to filter out the 800 nm components.

We demonstrated the generation of a spectrally flat supercontinuum with the same adaptive control scheme. We evaluated the flatness of the spectrum by the sum of the squares of the intensity differences between the adjacent digitized spectral components measured by the spectrometer. Figure 4(a) shows the supercontinuum spectrum obtained with the FTL pulse. The average power of the supercontinuum pulses is  $\sim 15$  mW. The Raman–Stokes component locates out of the spectral window. At 15 mW average input power, the central wavelength component is

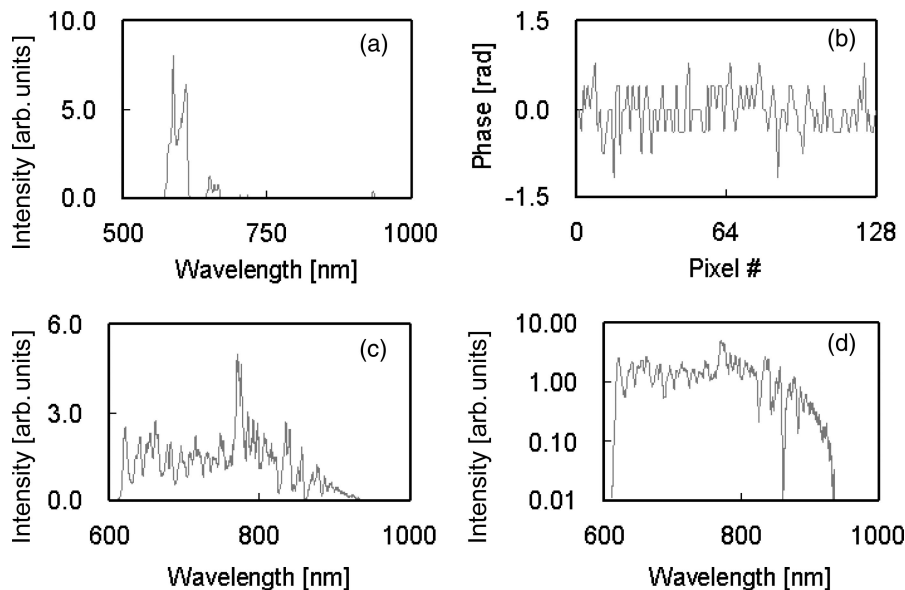


Fig. 4. (a) Supercontinuum spectrum obtained with the FTL pulse. The average power of the supercontinuum pulses is  $\sim 15$  mW. (b) Optimized phase modulation at SLM to obtain a flat supercontinuum spectrum. (c) Optimized flat supercontinuum spectrum plotted in the linear scale. (d) Same spectrum as that of (c) but plotted in the logarithm scale.

heavily suppressed and the anti-Stokes component is more enhanced. Figure 4(b) shows the optimized phase modulation at SLM, and Figs. 4(c) and 4(d) show the optimized flat supercontinuum spectrum in the linear and logarithm scales, respectively. The supercontinuum is expanded all the way from  $\sim 620$  to  $900$  nm. This result is very useful to use the supercontinuum pulse by selectively filtering only the peak excitation wavelengths required for a range of fluorescent samples. The spectral phase modulation shown in Fig. 4(b) to generate the flat supercontinuum exhibits no special feature.

We also tried to express the spectral phase  $\beta(\omega)$  of a laser pulse by a Taylor expansion with the four leading terms as in the following:

$$\beta(\omega) = \frac{1}{2!} \beta_2(\omega - \omega_0)^2 + \frac{1}{3!} \beta_3(\omega - \omega_0)^3 + \frac{1}{4!} \beta_4(\omega - \omega_0)^4 + \frac{1}{5!} \beta_5(\omega - \omega_0)^5. \quad (1)$$

Then the four dispersion coefficients  $\beta_k$  ( $k = 2-5$ ) were adopted as control parameters. These four coefficients were incremented at a single iterative optimization step using the SA, for example, with units of  $\Delta\beta_2 = \pm 1 \times 10^{-3}$  ps<sup>2</sup>,  $\Delta\beta_3 = \pm 1 \times 10^{-5}$  ps<sup>3</sup>,  $\Delta\beta_4 = \pm 1 \times 10^{-7}$  ps<sup>4</sup>, and  $\Delta\beta_5 = \pm 1 \times 10^{-9}$  ps<sup>5</sup>, respectively. However, we could not obtain any supercontinuum spectra with more uniform amplitude distribution than that shown in Fig. 4. Since the optical nonlinearity in the MSF is so complex that we have to increase the Taylor series to much higher orders to obtain the desired spectral distribution. It ultimately corresponds to individual manipulation of the spectral phase by 128 pixels of the SLM. To adaptively optimize the two-photon excitation processes with a designated supercontinuum pulse, the relative group

delay of each spectral component, in other words the spectral phase distribution, must be properly optimized together with the spectral amplitude distribution. Therefore for such a coherent control experiment we should use the pulse shaper with its maximum capability, although it will be more difficult to interpret physical insight from the optimized ultrashort laser pulse shapes. In the following adaptive pulse-shaping experiments, the 128 pixels of the SLM were individually controlled.

In general, supercontinuum spectra are always very much structured as shown in Fig. 4. Theoretical simulations of continuum generation have also predicted a deep and fine structure in the continuum spectra. They also predicted large variations in the spectral structure from small fraction input power. Gaeta reported that the variation of 0.1% in the input laser peak power is enough to cause a significant change in the spectral structure.<sup>22</sup>

#### B. Optimal Control of Two-Photon Fluorescence of Laser Dyes with Supercontinuum Pulses

The FTL pulse is always a bright pulse producing the highest multiphoton excitation if the two-photon excitation spectrum overlaps the laser spectrum. Therefore when we shape an excitation laser pulse with spectral phase modulation so that the highest two-photon fluorescence is obtained, it corresponds to compensation for residual dispersion of the laser pulse. If we place the pulse shaper after the MSF and adaptively shape the supercontinuum pulse to simultaneously obtain the highest two-photon fluorescence signals from various chromophores of which two-photon excitation spectra cover the entire spectrum of the supercontinuum pulse, we will be able to compress the supercontinuum pulse without measuring the pulse shape. In fact, the secondary dispersion of

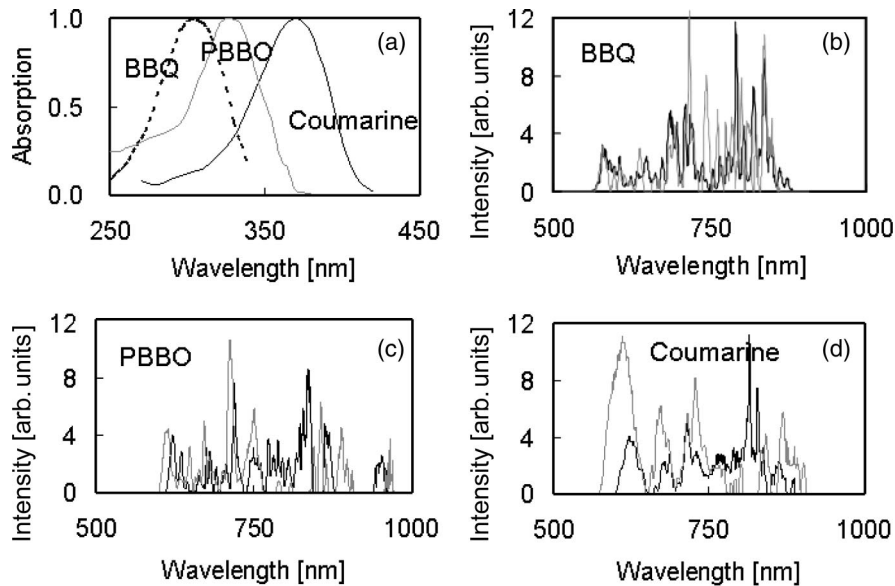


Fig. 5. (a) One-photon absorption spectrum of laser dye molecules of BBQ (dotted curve), PBBO (gray solid curve) and Coumarine 450 (black solid curve). Comparisons of supercontinuum spectra between the initial pulse (black solid curve) and the optimized (gray solid curve) pulse for (b) BBQ, (c) PBBO, and (d) Coumarine 450. Initial pulses were adjusted only with their secondary dispersion so that the highest fluorescence was obtainable.

the 30 cm MSFs used in our experiments is too large to compensate for the MSF dispersion only with the pulse shaper. An additional pulse compressor consisting of a pair of prisms is required.

When the pulse shaping is done prior to the pulse propagation through the MSF to maximize the two-photon fluorescence signal, both optical nonlinear processes of the fiber generating the supercontinuum and the two-photon excitation in the chromophores must be coherently controlled with the input laser pulse. Only for pulse propagation through fibers one can calculate a precompensation profile of the input pulse by solving a backward propagation equation to obtain the desired output pulse shapes from the fiber.<sup>23</sup> Although it is interesting to approach with such a numerical modeling for MSFs, in experiments adaptive pulse shaping should produce a bright supercontinuum pulse that produces the highest two-photon fluorescence.

We used three dye solutions and adaptively shaped the input laser pulses launched into the MSF to maximize the two-photon fluorescence with the self-learning optimization loop. The two-photon fluorescence was detected with a high-pass filter and a photomultiplier. When a FTL pulse is propagated through the MSF-A, the short wavelength bands corresponding to the anti-Stokes Raman is so strong that the signal-to-noise ratio for the two-photon fluorescence signal is degraded. Therefore prior to the adaptive pulse shaping, we adjusted the second-order dispersion of the input laser pulse by the pulse shaper to maximize the two-photon fluorescence signal. Since the optimization algorithm is sufficiently robust, the final optimization result, namely the fluorescence intensity, does not depend on the initial condition if the initial signal-to-noise ratio is high enough. Figure 5 shows the initial and optimized supercontinuum spectra for each dye solution to-

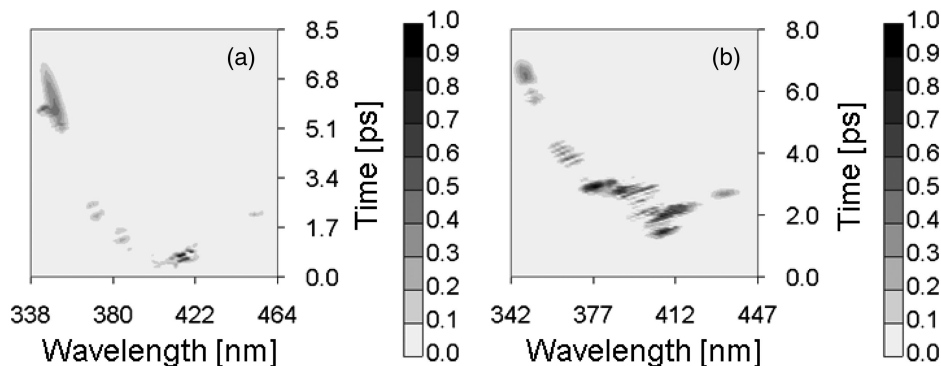


Fig. 6. XFROG traces for the supercontinuum pulse obtained with (a) before and (b) after the adaptive control done for a PBBO dye solution. The averaged supercontinuum power is 15 mW.

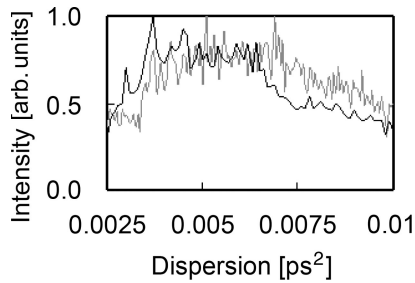


Fig. 7. Dependence of fluorescence intensity up on the secondary dispersion of the launched femtosecond laser pulse for EGFP fluorescent protein (black solid curve) and ECFP fluorescent protein (gray solid curve).

gether with one-photon excitation spectra. The initial second-order dispersion added to the FTL pulse is 0,  $0.97 \times 10^{-3}$ , and  $6.13 \times 10^{-3} \text{ ps}^2$  for BBQ, PBBO, and Coumarine 450, respectively. As a result of iterative pulse shaping, the two-photon fluorescence increases by factors of 2, 1.5, and 1.9 for BBQ, PBBO, and Coumarine 450 solutions, respectively, from the initial supercontinuum spectrum, which was obtained by manually adjusting the second-order dispersion.

We measured the optimized supercontinuum pulse profile with the XFROG method. The XFROG traces obtained for the supercontinuum pulse generated with a FTL pulse and the pulse optimized for two-photon excitation of PBBO are shown in Fig. 6. Since the optimized input laser pulse shape varies slightly at each optimization run, the FROG trace in Fig. 6 does not correspond to the spectrum of Fig. 5(c). The average input power was  $\sim 15 \text{ mW}$ . Since the MSF length is fairly long, significant group delay is observed through the entire spectral band. The group delay difference in the spectrum ranging from  $\sim 370$

to  $\sim 400 \text{ nm}$  is much decreased in the optimal supercontinuum. Since the sum wavelength is produced by the supercontinuum pulse with the  $800 \text{ nm}$  reference pulse, this spectral range corresponds to  $690\text{--}800 \text{ nm}$  of the supercontinuum. Compared with the two-photon excitation spectrum of PBBO, the supercontinuum pulse was shaped so that the intensity of the spectral components, which effectively contributes to the two-photon excitation, was enhanced, and at the same time the group delay dispersion in this spectral band of  $690\text{--}800 \text{ nm}$  is minimum.

### C. Selective Excitation of EGFP and ECFP with Shaped Supercontinuum Pulses

Finally, we simultaneously excited EGFP and ECFP protein molecules by supercontinuum pulses generated by the MSF-B and tried to enhance either one of two fluorescence signals. The absorption peak of these proteins is  $484 \text{ nm}$  and  $434 \text{ nm}$  for EGFP and ECFP, respectively. Therefore when exciting two proteins simultaneously with supercontinuum pulse, we obtain two-photon fluorescence from both proteins. Figure 7 shows the variation of the two-photon fluorescence signal for various second-order positive dispersions added to the FTL input laser pulse. It is shown that the fluorescence ratio of ECFP and EGFP slightly improved as the second-order dispersion increased. Figure 8 shows the evolution of the fluorescence ratio during iterative optimization control. The initial input pulse was set as the FTL pulse. When the input laser pulse was adaptively controlled so that the fluorescence ratio of EGFP and ECFP is highest, we obtained the enhancement factor of  $\sim 1.8$  relative to the initial condition after  $\sim 500$  iterative loops. On the other hand, when the control parameter was set to the fluorescence ratio of ECFP and EGFP,

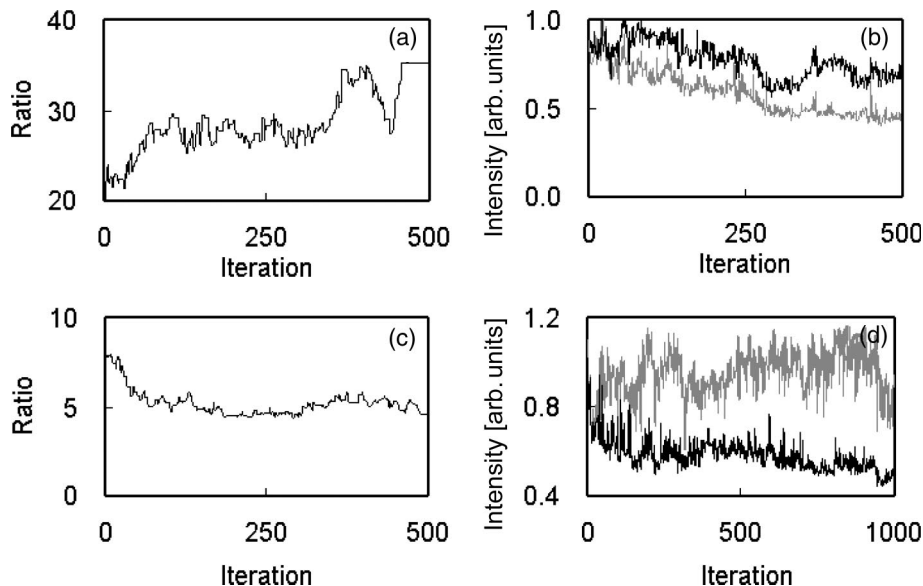


Fig. 8. Results of adaptive control of the supercontinuum spectrum so that the highest fluorescence intensity ratio is obtainable. (a) Evolution of fluorescence ration EGFP/ECFP during adaptive control. (b) Evolution of fluorescence intensity of EGFP (black solid curve) and ECFP (gray solid curve). (c) Evolution of fluorescence ration ECFP/EGFP during adaptive control. (d) Evolution of fluorescence intensity of EGFP (black solid curve) and ECFP (gray solid curve).

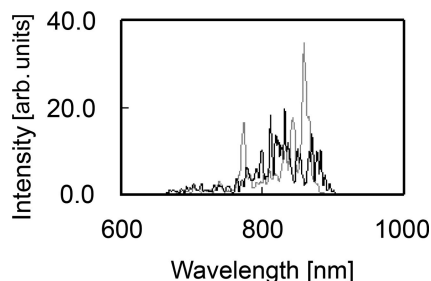


Fig. 9. Optimized supercontinuum spectra to attain the highest EGFP/ECFP fluorescence intensity ratio (black solid curve) and to attain the highest ECFP/EGFP fluorescence intensity ratio (gray solid curve).

the enhancement factor of  $\sim 1.9$  relative to the initial condition was obtained. Figure 9 shows the optimized supercontinuum spectra obtained at each the optimization ran.

In theory, when the SH spectrum of the supercontinuum pulse is shaped so that most of the SH power is concentrated to the spectral band where the two-photon excitation spectrum ratio between two proteins show the highest value,<sup>2-4</sup> the highest distinguishable ratio is obtainable between the two proteins. Then we will be able to modify our adaptive spectrum shaping scheme of the first experiment in this paper. Instead of the supercontinuum spectrum, we can feed back a fraction of the SH spectral power concentrated in the desired SH spectral band. However, in protein molecules, exhibiting broad two-photon excitation spectra, there may be various energy relaxation passes before populating the energy levels emitting fluorescence. Dumping as well as excited state absorption will take place by some of wavelengths in the supercontinuum pulse. The adaptive pulse shaping referring the fluorescence signal can take account of those processes without prior knowledge of the complex kinetics among the excitation manifolds.

#### 4. Conclusion

In this paper we showed the flexibility in the supercontinuum spectra from the MSF using adaptive input pulse shape control. This scheme was extended to design the optimal input laser pulse so that the supercontinuum pulse from the MSF can produce the highest two-photon fluorescence or the highest contrast ratio between two different fluorescence proteins. The adaptive control scheme optimized simultaneously both the optical nonlinearity of the fiber and the two-photon excitation processes in the proteins. To our knowledge this is the first demonstration that the supercontinuum spectrum generated via coherent control by the shaped input pulse was applied for nonlinear interaction of light and matter. First, from the two-photon microscopy viewpoint, this pulse shaping prior to the pulse propagation in the fiber can exclude the spatiotemporal coupling effect that all pulse-shaping experiments using segmented SLMs suffer. Second, since the shaped pulse is produced directly from the fiber output, the

fiber acts as an optical guide to the microscope. Since the highly functional supercontinuum pulses are available with our scheme from a single mode-lock laser, multicolor two-photon imaging is available without an optical parametric oscillator.

#### References

1. A. M. Weiner, "Femtosecond pulse shaping using spatial light modulators," *Rev. Sci. Instrum.* **71**, 929–1960 (2000).
2. K. A. Walowicz, I. Pastirk, V. V. Lozovoy, and M. Dantus, "Multiphoton intrapulse interference. I. Control of multiphoton processes in condensed phases," *J. Phys. Chem. A* **106**, 9369–9373 (2002).
3. V. V. Lozovoy, I. Pastirk, K. A. Walowicz, and M. Dantus, "Multiphoton intrapulse interference. II. Control of two- and three-photon laser induced fluorescence with shaped pulses," *J. Chem. Phys.* **118**, 3187–3196 (2003).
4. I. Pastirk, J. M. D. Cruz, K. A. Walowicz, V. V. Lozovoy, and M. Dantus, "Selective two-photon microscopy with shaped femtosecond pulses," *Opt. Express* **11**, 1695–1701.
5. J. P. Ogilvie, K. J. Kubarych, A. Alexandrou, and M. Joffre, "Fourier transform measurement of two-photon excitation spectra: applications to microscopy and optimal control," *Opt. Lett.* **30**, 911–913 (2005).
6. A. Assion, T. Baumert, M. Bergt, T. Brixner, B. Kiefer, V. Seyfried, M. Strehle, and G. Gerber, "Control of chemical reactions by feedback-optimized phase-shaped femtosecond laser pulses," *Science* **282**, 919–922 (1998).
7. H. Kawano, Y. Nabekawa, A. Suda, Y. Oishi, H. Mizuno, A. Miyawaki, and K. Midorikawa, "Attenuation of photobleaching in two-photon excitation fluorescence from green fluorescent protein with shaped excitation pulses," *Biochem. Biophys. Res. Commun.* **311**, 592–596 (2003).
8. J. K. Ranka, R. S. Windeler, and A. J. Stentz, "Visible continuum generation in air-silica microstructure optical fibers with anomalous dispersion at 800 nm," *Opt. Lett.* **25**, 25–27 (2000).
9. V. Nagarajan, E. Johnson, P. Schellenberg, W. Parson, and R. Windeler, "A compact versatile femtosecond spectrometer," *Rev. Sci. Instrum.* **73**, 4145–4149 (2002).
10. H. N. Paulsen, K. M. Hilligsoe, J. Thogersen, S. R. Keiding, and J. J. Larsen, "Coherent anti-Stokes Raman scattering microscopy with a photonic crystal fiber light source," *Opt. Lett.* **28**, 1123–1125 (2003).
11. H. Kano and H. Hamaguchi, "Femtosecond coherent anti-Stokes Raman scattering spectroscopy using supercontinuum generated from a photonic crystal fiber," *Appl. Phys. Lett.* **85**, 4298–42300 (2004).
12. T. W. Kee and M. T. Cicerone, "Simple approach to one-laser, broadband coherent anti-Stokes Raman scattering spectroscopy," *Opt. Lett.* **29**, 2701–2703 (2004).
13. S. O. Konorov, D. A. Akimov, A. A. Ivanov, M. V. Alifimov, and A. M. Zhelyikov, "Microstructure fibers as frequency tunable sources of ultrashort chirped pulses for coherent nonlinear spectroscopy," *Appl. Phys. B* **78**, 565–567 (2004).
14. B. von Vacano, W. Wohlleben, and M. Motzkus, "Actively shaped supercontinuum from a photonic crystal fiber for nonlinear coherent microscopy," *Opt. Lett.* **31**, 413–415 (2006).
15. T. Tanabe, H. Tanabe, Y. Teramura, and F. Kannari, "Spatio-temporal measurements based on spatial spectral interferometry for ultrashort optical pulses shaped by a Fourier pulse shaper," *J. Opt. Soc. Am. B* **19**, 2795–2802 (2002).
16. T. Tanabe, F. Kannari, F. Korte, J. Koch, and B. Chichkov, "Influence of spatiotemporal coupling induced by an ultrashort laser pulse shaper on a focused beam profile," *Appl. Opt.* **44**, 1092–1098 (2005).
17. M. Tianprateep, J. Tada, and F. Kannari, "Influence of polarization and pulse shape of femtosecond initial laser pulses on

- spectral broadening in microstructure fibers," *Opt. Rev.* **12**, 179–189 (2005).
18. S. Xu, D. H. Reitze, and R. S. Windeler, "Controlling nonlinear processes in microstructured fibers using shaped pulses," *Opt. Express*. **12**, 4731–4741 (2004).
  19. D. TÜRke, W. Eohlleben, J. Teipel, M. Motzkus, B. Kibler, J. Dudley, and H. Giessen, "Chirp-controlled soliton fission in tapered optical fibers," *Appl. Phys. B* **83**, 47–42 (2006).
  20. M. Tianprateep, J. Tada, T. Yamazaki, and F. Kannari, "Spectral-shape-controllable supercontinuum generation in microstructured fibers using adaptive pulse shaping technique," *Jpn. J. Appl. Phys.* **43**, 8059–8063 (2004).
  21. M. Sato, M. Suzuki, M. Shiozawa, T. Tanabe, K. Ohno, and F. Kannari, "Adaptive pulse shaping of femtosecond laser pulses in amplitude and phase through a single-mode fiber by referring to frequency-resolved optical gating patterns," *Jpn. J. Appl. Phys.* **41**, 3704–3709 (2002).
  22. A. L. Gaeta, "Nonlinear propagation and continuum generation in microstructured optical fiber," *Opt. Lett.* **27**, 924–926 (2002).
  23. T. Yamazaki, T. Tanabe, F. Kannari, Y. Shida, and S. Fushimi, "Fiber delivery of ultrashort optical pulses preshaped on the basis of a backward propagation solver," *Jpn. J. Appl. Phys.* **42**, 7313–7317 (2003).